PHYSICAL REVIEW B VOLUME 50, NUMBER 24 15 DECEMBER 1994-II

Theory of Rabi splitting in cavity-embedded quantum wells

Stefan Jorda
Institut für Theoretische Physik, Universität Regensburg, D-93040 Regensburg, Federal Republic of Germany
(Received 21 September 1994)

We present a quantum theory of interaction between quantum-well excitons and electromagnetic eigenmodes of a multilayer dielectric cavity. The coupled exciton-photon modes are obtained by analyzing the exciton spectral function. The design of the cavity allows us to obtain enhanced spontaneous emission or a normal-mode splitting. We find very good agreement with the normal-mode splitting data of Weisbuch *et al.* [Phys. Rev. Lett. **69**, 3314 (1992)].

Embedding quantum wells (QW's) in semiconductor microcavities has opened an interesting field in the study of the interaction of both confined excitons and photons. Through the design of QW's and dielectric mirrors the excitonic resonance position as well as the dispersion and linewidth of the cavity quasimodes can be tailored almost at will, leading to a larger variety of phenomena than known from the well-understood bulk system. In bulk material photons have a vanishing linewidth and a simple linear dispersion determined by the speed of light in the medium. For fixed polarization an exciton state with given wave vector $\mathbf{Q}$ can interact with only exactly one photon state determined by conservation of momentum. As a result two normal modes, the radiatively stable polaritons, arise. In two dimensional systems, generally speaking, the momentum is conserved only in the plane of the layers, thus a dipole allowed exciton may couple to a whole continuum of photon states. As a result, as shown for a simple QW, radiatively unstable polariton states arise.[1–4] With increasing reflectivity of the mirrors in a dielectric cavity the continuum of photon modes "condenses" into Fabry-Pérot quasimodes which have a finite linewidth. Roughly speaking, the following two limiting situations occur: If the linewidth is larger than the expected normal-mode splitting (the so-called weak coupling case), the spontaneous emission of the exciton will be enhanced at the crossing point between exciton and cavity mode. If, in contrast, the linewidth is smaller than the expected splitting (the strong coupling case), two split normal modes arise which are radiatively unstable. Enhanced spontaneous emission has been reported experimentally by Ochi *et al.*[5] and Yamamoto *et al.*,[6] whereas normal-mode splitting has been observed by Weisbuch *et al.*[7] and Houdré *et al.*[8]

So far, most of the theoretical investigations concerning modified spontaneous emission[9–11] or the transition between modified spontaneous emission and normal-mode splitting[12,13] have dealt with cavity-embedded localized point dipoles. Citrin[14] pointed out that these calculations missed the extended nature of the exciton state and the related strongly $Q_\parallel$-dependent properties ($Q_\parallel$ being the in-plane wave vector). In Ref. 14, the transition between modified spontaneous emission and normal-mode splitting was discussed for a cavity consisting of two planar metallic mirrors. Savona *et al.*[15] considered the case of perfectly reflecting metallic mirrors and fitted the value of the excitonic oscillator strength to the experimental values of Ref. 7. This model, due to the vanishing linewidth of the cavity modes, is equivalent to a simple interacting two-level system and predicts a normal-mode splitting for any interaction strength, in contrast to experiments. Weisbuch *et al.*[7] modeled their experimental results with an analysis introduced by Zhu *et al.*[16] where the linewidth of the cavity and the exciton features were introduced as input parameters. Thus, at present, no theoretical results based on a realistic and parameter-free description of the multilayer cavities exist.

In this paper we present the quantum theory of interaction between QW excitons and electromagnetic eigenmodes of a multilayer dielectric cavity. These cavities consist typically of a central layer surrounded by two distributed Bragg reflectors (DBR's), each consisting of a stack of alternating quarter-wave layers of two dielectrics. The dielectric constant is therefore a piecewise constant function of the z coordinate (the z axis will be taken as growth direction). The experiment of Ref. 7 is a normal-incidence reflectivity experiment ($Q_\parallel=0$) where only T polarized excitons interacting with TE electromagnetic modes can be excited. At $Q_\parallel=0$ the electromagnetic normal modes of such a structure are described by properly matched right and left traveling plane waves (with respect to z) which serve as a basis for the expansion of the vector potential (exponentially decaying modes can occur only at $Q_\parallel \neq 0$). Experimental samples are, in general, not symmetric with respect to z, due to the interface to air on one side and an interface to the substrate on the other side. However, in the sample of Ref. 7, to which all our numerical results will refer, the reflectivities of the two mirrors were balanced by using different numbers of quarter-wave layers on each side. Therefore it is justified to restrict the theory to symmetrical structures. In addition, for a single QW or an array of QW's placed symmetrically with respect to the center of the structure, only the even electromagnetic modes interact with the excitons, which allows a reduction of the basis set.

With these simplifications the vector potential can be expanded in terms of creation and annihilation operators for electromagnetic modes ($c_\rho^\dagger, c_\rho$) as[20]

$$A_y(\mathbf{r})=\sum_\rho \left(\frac{2\pi\hbar c^2}{\bar{\omega}_\rho \varepsilon_s\, \theta \mathscr{A}\mathscr{L}}\right)^{1/2} (c_\rho+c_\rho^\dagger)\ R(z) \ , \quad (1)$$

where we have chosen the polarization parallel to $\hat{e}_y$. The modes with $Q_\parallel=0$ but different energy can be distinguished by ρ which corresponds to Q_z in the surrounding medium characterized by the dielectric constant ε_s. $\tilde{\omega}_\rho = c\rho/\sqrt{\varepsilon_s}$ is the frequency of the modes, $R(z)$ is the properly matched linear combination of right and left traveling plane waves, and $\mathscr{A}$ ($\mathscr{L}$) is a normalization area (length). θ is the normalization constant of the electromagnetic modes which is given by $|A_s|^2+|B_s|^2$, where A_s and B_s are the field amplitudes in the surrounding layers. This result is derived in Ref. 17 for a simple waveguide structure and can be generalized to more complicated structures by induction. A_s and B_s are related to the amplitudes at the interface central-layer/DBR, A_c and B_c, by a transfer matrix, which incorporates the proper boundary conditions at the interfaces. The relation

$$\begin{pmatrix} A_s \\ B_s \end{pmatrix} = M \begin{pmatrix} A_c \\ B_c \end{pmatrix} = \frac{1}{2} M \begin{pmatrix} \exp(i\phi_c) \\ \exp(-i\phi_c) \end{pmatrix} \tag{2}$$

holds, where $\phi_c = \sqrt{\varepsilon_c}\,\omega\, l_c/c$ with ε_c the dielectric constant of the central layer and l_c half its width. The 2×2 transfer matrix M is given by[18,19]

$$M = D_s^{-1} T^N D_c \ . \tag{3}$$

N is the number of pairs of quarter-wave layers and the matrix T, which describes the transmission through one pair of them, is given by

$$T = \begin{pmatrix} T_{11} & iT_{12} \\ iT_{21} & T_{22} \end{pmatrix} = D_2 P_2 D_2^{-1} D_1 P_1 D_1^{-1} \ . \tag{4}$$

The matrices D_i are the dynamical matrices and P_i the propagation matrices for the ith layer. They are given by[18,19]

$$D_i = \begin{pmatrix} 1 & 1 \\ n_i & -n_i \end{pmatrix} \ , \tag{5}$$

$$P_i = \begin{pmatrix} \exp(i\phi_i) & 0 \\ 0 & \exp(-i\phi_i) \end{pmatrix} \ , \tag{6}$$

where n_i is the index of refraction in the ith layer and the phases ϕ_i are given by $\phi_i = \sqrt{\varepsilon_i}\,\omega\, l_i/c$ with the layer thickness l_i. As T is a unimodular matrix the Nth power can be evaluated using the Chebyshev identity to be

$$T^N = \begin{pmatrix} T_{11} U_{N-1}(x) - U_{N-2}(x) & iT_{12} U_{N-1}(x) \\ iT_{21} U_{N-1}(x) & T_{22} U_{N-1}(x) - U_{N-2}(x) \end{pmatrix}, \tag{7}$$

where $x = 1/2\,(T_{11}+T_{22})$ and $U_N(x)$ are the Chebyshev polynomials defined by

$$U_N(x) = \frac{\sin[(N+1)\arccos x]}{\sqrt{1-x^2}} \ . \tag{8}$$

For $x>1$ a similar relation with hyperbolic instead of trigonometric functions holds. With the expansion (1) the expression for the electromagnetic field energy $(1/8\pi)\int(\mathbf{E}\cdot\mathbf{D}+B^2)\,dV$ reduces to $H_{\rm em} = \sum_\rho \hbar\tilde{\omega}_\rho c_\rho^\dagger c_\rho$.

The exciton-photon interaction can be derived from the terms linear and quadratic in the vector potential by the procedure described in Refs. 3 and 20. It yields the expressions

$$H_{\rm int}^{(1)} = \sum_\rho C_\rho (c_\rho + c_{-\rho}^\dagger)(B^\dagger + B) \ , \tag{9}$$

$$H_{\rm int}^{(2)} = \sum_{\rho\rho'} \frac{C_\rho C_{\rho'}}{\hbar\Omega_{\rm ex}} (c_\rho^\dagger + c_{-\rho})(c_{\rho'} + c_{-\rho'}^\dagger) \ , \tag{10}$$

where $B^\dagger$ (B) is an exciton creation (annihilation) operator and the coupling constant is

$$C_\rho = \left(\frac{2\pi\hbar}{c\rho\sqrt{\varepsilon_s}\,\theta\,\mathscr{L}} \right)^{1/2} \mu\,\Omega_{\rm ex}\,\phi(0) O(\rho) \ . \tag{11}$$

Here μ is the dipole matrix element $e\langle c|x|x\rangle$ between the bulk band-edge Bloch states for conduction ($|c\rangle$) and valence band ($|v\rangle$) and $\Omega_{\rm ex}$ is the exciton frequency. $\phi(0)$ is the exciton relative function at vanishing electron-hole separation in the QW. The function $O(\rho)$ is a measure of the overlap between QW subband functions and electromagnetic modes. It will be given explicitly further below.

The Hamiltonian for the coupled exciton radiation system can now be written as

$$H = \hbar\Omega_{\rm ex} B^\dagger B + H_{\rm em} + H_{\rm int}^{(1)} + H_{\rm int}^{(2)} \ . \tag{12}$$

Hamiltonian (12) can be diagonalized exactly by solving the corresponding Heisenberg equations,[3] by the generalized Hopfield transformation,[15,20] or by summing the Dyson series.[4,14] Any of these equivalent procedures yields the exciton self-energy

$$\Sigma(\omega) = \frac{\omega^2}{\Omega_{\rm ex}^2} \sum_\rho \frac{2\tilde{\omega}_\rho |C_\rho|^2}{\hbar[(\omega+i\delta)^2 - \tilde{\omega}_\rho^2]} O^2(\rho) \ , \tag{13}$$

with real part

$$\mathrm{Re}\,\Sigma(\omega) \;=\; -\frac{4\mu^2\omega^2}{c^2}\phi^2(0) \int_0^\infty \frac{d\rho}{\rho^2 - \varepsilon_s\omega^2/c^2} \frac{1}{\theta} O^2(\rho) \ , \tag{14}$$

and imaginary part

$$\mathrm{Im}\,\Sigma(\omega) = \frac{2\pi\mu^2\omega}{\sqrt{\varepsilon_s}c} \frac{1}{\theta} \phi^2(0)\, O^2(\rho) \ . \tag{15}$$

As shown in Ref. 20 the integration in Eq. (14) can be done analytically for a simple waveguide. For the complicated structure discussed here no closed expression for $\mathrm{Re}\,\Sigma(\omega)$ could be found. Therefore the integration in Eq. (14) was performed numerically. In addition, we also used an approximation for θ which could be handled analytically. This approximation consists in neglecting the variation of the phases ϕ_1 and ϕ_2 in the DBR layers for different energies and setting $\phi_1 = \phi_2 = \pi/2$. In this case θ reduces to

$$\theta = \left(\frac{\varepsilon_1}{\varepsilon_2}\right)^N \cos^2\phi_c + \frac{\varepsilon_c}{\varepsilon_s}\left(\frac{\varepsilon_2}{\varepsilon_1}\right)^N \sin^2\phi_c \ , \tag{16}$$

where ε_1 and ε_2 are the dielectric constants of the DBR layers. This expression is proportional to the corresponding expression in a simple waveguide with an effective dielectric constant of the surrounding medium given by $\tilde{\varepsilon}_s = \varepsilon_s(\varepsilon_1/\varepsilon_2)^{2N}$.[20] Therefore, using Eq. (16), $\mathrm{Re}\,\Sigma(\omega)$ can be evaluated by standard contour integration and summation of the contributions of the infinite number of poles, as described in the Appendix of Ref. 20. As result we obtain

$$\mathrm{Re}\,\Sigma(\omega)=\frac{2\pi\mu^2\omega}{c\sqrt{\varepsilon_c}}\frac{(1-\alpha)\sin\phi_c\cos\phi_c}{\sin^2\phi_c+\alpha\cos^2\phi_c}\;\phi^2(0)\,O^2(\rho)\;, \tag{17}$$

where $\alpha=(\varepsilon_s/\varepsilon_c)(\varepsilon_1/\varepsilon_2)^{2N}$. As a check for the numerical integration which requires a large number of grid points due to the oscillating behavior of the integrand, we also evaluated Eq. (14) numerically using Eq. (16). A very good agreement was obtained.

The spectrum of the coupled exciton-photon excitations [i.e., position and linewidth of the exciton (the two polariton branches) in the weak (strong) coupling case] is given by the exciton spectral function defined by[21]

$$A^{\mathrm{ex}}(\omega)=-2\;\mathrm{Im}G^{\mathrm{ret}}(\omega)$$

$$\propto\frac{\mathrm{Im}\,\Sigma(\omega)}{[\omega-\Omega_{\mathrm{ex}}-\mathrm{Re}\,\Sigma(\omega)]^2+[\mathrm{Im}\,\Sigma(\omega)]^2}\;, \tag{18}$$

where $G^{\mathrm{ret}}(\omega)$ is the retarded exciton Green's function.

Similarly, the bare cavity modes are determined by the bare photon spectral function. It is straightforward to show that

$$A^{\mathrm{photon}}(\omega)\propto\mathrm{Im}\sum_\rho\frac{|S_\rho|^2}{\hbar[(\omega+i\delta)^2-\bar{\omega}_\rho^2]}\propto\frac{1}{\theta}\;, \tag{19}$$

where S_ρ is the expansion coefficient in Eq. (1). Therefore a numerical analysis of $1/\theta$ reveals the cavity mode structure. For the approximate θ given in Eq. (16) position and linewidth of the cavity modes can be given analytically. The real part of the cavity frequency is the same as in the metallic cavity of Ref. 15, but due to the finite linewidth this approximation goes beyond Ref. 15.

The samples investigated in Ref. 7 consisted of an odd number (1–7) of GaAs QW's of width L = 75 Å with a HH exciton resonance at $\hbar\Omega_{\mathrm{ex}}=1583$ meV. These QW's were $L_B=100$ Å apart and the whole array placed at the center of a wedge shaped layer of $Al_{0.2}Ga_{0.8}As$. The DBR's were formed by alternating $\lambda/4$ layers of AlAs and $Al_{0.4}Ga_{0.6}As$, where λ was adjusted to the exciton frequency ($\lambda=2\pi v/\Omega_{\mathrm{ex}}$, v is the speed of light in the individual layers). The width of the $\lambda/4$ layers was constant throughout the sample. The whole structure was grown on a GaAs substrate. The wedge shaped central layer had a width around λ and allowed for a tuning or detuning of cavity and exciton frequency by probing different spots of the sample. For the numerical calculations we used the values (for $\hbar\omega=1.6$ eV) $\varepsilon_c=11.78$ (corresponding to $Al_{0.2}Ga_{0.8}As$), $\varepsilon_1=8.76$ (AlAs), $\varepsilon_2=11.02$ ($Al_{0.4}Ga_{0.6}As$) and $\varepsilon_s=12.53$ (GaAs).[22] For the HH exciton oscillator strength f, which is related to the quantities μ and $\phi(0)$ by $\mu^2\phi^2(0)=(\hbar e^2/2mE_g)f$, we took the value $f=32.9\times10^{-5}$ Å^{-2}. This value for the oscillator strength was obtained by solving the momentum-space two-particle Schrödinger equation including LH-HH mixing with a modified quadrature method.[23] For a sample with an odd number n_{QW} of QW's that are placed symmetrically with respect to the sample center the function $O^2(\rho)$ is given by

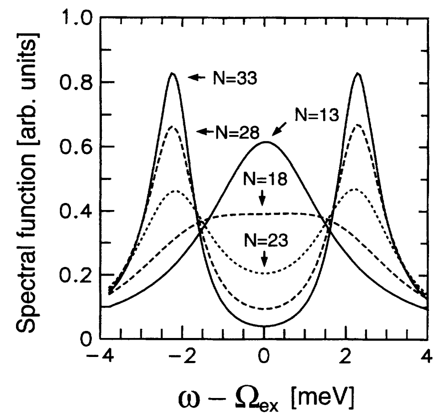

FIG. 1. Spectral function for different numbers N of pairs of quarter-wave layers in the DBR's. The situation corresponds to coinciding exciton and cavity frequency.

$$O^2(\rho)=\sum_{k=-(n_{\mathrm{QW}}-1)/2}^{(n_{\mathrm{QW}}-1)/2}\cos^2\left(\sqrt{\frac{\varepsilon_c}{\varepsilon_s}}k\,\rho\,(L+L_B)\right). \tag{20}$$

This term is a constant if we neglect the weak dependence on ω and set $\rho=\sqrt{\varepsilon_s}\,\Omega_{\mathrm{ex}}/c$. Under this condition it can be interpreted as an effective number n_{eff} of QW's.[15] It equals 1 for $n_{\mathrm{QW}}=1$, 2.62 for $n_{\mathrm{QW}}=3$, 3.38 for $n_{\mathrm{QW}}=5$, and 3.47 for $n_{\mathrm{QW}}=7$. There is a saturation for large n because the additional QW's have to be placed further away from the antinode position of the cavity mode where the overlap is large. This saturation has been seen in Ref. 7.

In Fig. 1 we present numerical results for the spectral function for different numbers of DBR layers as a function of ω. The width of the central layer which comprises an array of five QW's is λ and therefore $\Omega_{\mathrm{ex}}=\Omega_{\mathrm{cav}}$. In addition a phenomenological exciton damping of $\gamma=1$ meV was introduced. For $N=13$ the spectrum consists of one broad peak corresponding to enhanced spontaneous emission. A similar sample was investigated in Ref. 6. As N increases, the linewidth of the cavity mode decreases and two split normal modes emerge. This is the situation corresponding to the ex-

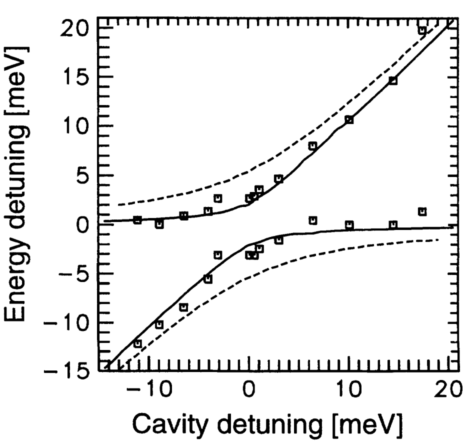

FIG. 2. Energy detuning of the normal modes relative to $\hbar\Omega_{\mathrm{ex}}$ versus cavity detuning $\hbar\Omega_{\mathrm{cav}}-\hbar\Omega_{\mathrm{ex}}$. Dashed lines correspond to the analytical approximation, full lines to the full calculation.

periments of Ref. 7. Next we fixed $N=33$ and varied the width of the central layer. The position of the bare cavity mode was determined by the maxima of $1/\theta$ and the positions of the split normal modes by the maxima of $A^{ex}(\omega)$. Figure 2 shows the positions of the normal modes relative to $\hbar\Omega_{ex}$ versus the cavity detuning $\hbar\Omega_{cav}-\hbar\Omega_{ex}$. The full lines show the results for the full calculation which agree very well with the experimental results of Ref. 7 shown as squares. The dashed lines correspond to the analytical approximation which clearly overestimates the level splitting. In order to reproduce the experimental data within this approximation a value of $fn_{eff}=31\times10^{-5}$ Å^{-2} has to be used, as is the case in the theory of Ref. 15.

In conclusion we have presented an accurate theoretical explanation for the experimentally observed exciton-photon mode splitting in cavity-embedded QW's. We have shown that, whereas the normal-mode splitting can be predicted qualitatively by a simple interacting two-level system, a theory which describes properly the transition between enhanced spontaneous emission and normal-mode splitting requires a complete description of the multilayer mirrors. Recently angle resolved luminescence experiments have been performed which extend the experiments of Ref. 7 to the case $Q_\parallel \neq 0$.[24] It is straightforward to extend the presented theory to this case.

I am grateful to U. Rössler for continuous support and a critical reading of the manuscript. Stimulating discussions with V. Savona, Z. Hradil, A. Quattropani, and R. P. Stanley are acknowledged. Thanks is also given to R. Winkler for the calculation of the oscillator strength.

[1] V.M. Agranovich and O.A. Dubovskii, Pis'ma Zh. Eksp. Teor. Fiz. **3**, 345 (1966) [JETP Lett. **3**, 223 (1966)].
[2] F. Tassone, F. Bassani, and L.C. Andreani, Nuovo Cimento D **12**, 1673 (1990); Phys. Rev. B **45**, 6023 (1992).
[3] S. Jorda, U. Rössler, and D. Broido, Phys. Rev. B **48**, 1669 (1993); Superlatt. Microstruct. **12**, 85 (1992).
[4] D.S. Citrin, Phys. Rev. B **47**, 3832 (1992).
[5] N. Ochi, T. Shiotani, M. Yamanishi, Y. Honda, and I. Suemune, Appl. Phys. Lett. **58**, 2735 (1991).
[6] Y. Yamamoto, S. Machida, Y. Horikoshi, K. Igeta, and G. Björk, Opt. Commun. **80**, 337 (1991).
[7] C. Weisbuch, M. Nishioka, A. Ishikawa, and Y. Arakawa, Phys. Rev. Lett. **69**, 3314 (1992).
[8] R. Houdré, R.P. Stanley, U. Oesterle, M. Ilegems, and C. Weisbuch, J. Phys. (Paris) Colloq. **54**, C5-51 (1993); Phys. Rev. B **49**, 16 761 (1994).
[9] S.G. Brorson, H. Yokoyama, and E.P. Ippen, IEEE J. Quantum Electron. **QE-26**, 1492 (1990).
[10] G. Björk, S. Machida, Y. Yamamoto, and K. Igeta, Phys. Rev. B **44**, 669 (1991).
[11] S.T. Ho, S.L. McCall, and R.E. Slusher, Opt. Lett. **18**, 909 (1993).
[12] S. Sachdev, Phys. Rev. A **12**, 148 (1984).
[13] Xiao-Ping Feng and Kikuo Ujihara, Phys. Rev. A **41**, 2668 (1990).
[14] D.S. Citrin, IEEE J. Quantum Electron. **QE-30**, 997 (1994).
[15] V. Savona, Z. Hradil, A. Quattropani, and P. Schwendimann, Phys. Rev. B **49**, 8774 (1994).
[16] Y. Zhu, D.J. Gauthier, S.E. Morin, Q. Wu, H.J. Carmichael, and T.W. Mossberg, Phys. Rev. Lett. **64**, 2499 (1990).
[17] D. Marcuse, *Theory of Dielectric Optical Waveguides* (Academic Press, New York, 1974).
[18] M. Born and E. Wolf, *Principles of Optics* (Pergamon Press, Oxford, 1970).
[19] P. Yeh, *Optical Waves in Layered Media* (John Wiley & Sons, New York, 1988).
[20] S. Jorda, Phys. Rev. B **50**, 2283 (1994).
[21] G.D. Mahan, *Many-Particle Physics* (Plenum Press, New York, 1990).
[22] *Semiconductors. Physics of Group IV Elements and III-V Compounds,* edited by O. Madelung, M. Schulz, and H. Weiss, Landolt-Börnstein, New Series, Group 3, Vol. 17, Pt. a (Springer-Verlag, Berlin, 1982).
[23] R. Winkler, S. Jorda, and U. Rössler, in *Physics of Semiconductors—Proceedings of the XXII International Conference* , edited by D. J. Lockwood (World Scientific, Singapore, in press).
[24] R. Houdré, C. Weisbuch, R.P. Stanley, U. Oesterle, P. Pallandini, and M. Ilegems, Phys. Rev. Lett. **73**, 2043 (1994).